

IV. Disks, Winds, and Magnetic Fields

HUBBLE SPACE TELESCOPE IMAGING OF THE DISKS AND JETS OF TAURUS YOUNG STELLAR OBJECTS

KARL STAPELFELDT

*Jet Propulsion Laboratory, California Institute of Technology
4800 Oak Grove Drive, Mail Stop 183-900
Pasadena CA 91109, USA*

CHRISTOPHER J. BURROWS

Space Telescope Science Institute

JOHN E. KRIST

Space Telescope Science Institute

AND

THE WFPC2 SCIENCE TEAM

Abstract. We report on Hubble Space Telescope imaging of eleven young stellar objects in the nearby Taurus molecular clouds. The high spatial resolution and stable point spread function of HST reveal important new details of the circumstellar nebulosity of these objects. Three sources (HH 30, FS Tau B, and DG Tau B) are resolved as compact bipolar nebulae without a directly visible star. In all three cases, jet widths near the sources are found to be 50 AU or less. Flattened disk structures are seen in absorption in HH 30 and FS Tau B, and in reflection about GM Aur. Extended envelope structures traced by scattered light are present in HL Tau, T Tau, DG Tau, and FS Tau. The jet in DG Tau exhibits a large opening angle and is already resolved into a bow-like structure less than 3'' from the star.

1. Introduction

The environment of a young stellar object (YSO) is a complex region where disks, infalling envelopes, outflows, and companion stars interact to define the distribution of circumstellar material. Of particular interest are the properties of protoplanetary disks believed to be present during these first stages of stellar evolution. In combination with spectral energy distributions

and kinematics derived from spectroscopy, high resolution optical imaging can greatly clarify the geometry and dynamical state of material in the YSO environment. For nearby sources such as those associated with the Taurus molecular clouds, optical images with the Hubble Space Telescope / Wide Field and Planetary Camera 2 (HST/WFPC2) provide a typical linear resolution of 10 AU. This capability has led to important new discoveries since the repair of HST, and offers exciting prospects for future work. In this contribution, we review YSO imaging results obtained in Guaranteed Time Observation programs by the WFPC2 Science Team as of early 1997.

2. Observations

All the targets are low-mass pre-main sequence stars located in Taurus-Auriga at a distance of 140 pc. They were observed using broadband V, R, and I filters, usually on the Planetary Camera. Typically both short (10-30 sec) and long (200-600 sec) exposures were made in each filter, and the full sequence was completed in a single HST orbit. Emission lines from Herbig-Haro objects occur primarily in the R bandpass, and are largely absent in the I bandpass. A comparison of these two images thus allows HH objects to be distinguished from reflection nebulosity. This procedure has worked well except very close to bright objects such as DG Tau, where noise from the background continuum limits the visibility of jet features.

3. Results for Point Sources with Adjacent Nebulosity

These bright stars were deliberately saturated to provide maximum dynamic range for detection of circumstellar features. Reference point spread functions from both HST observations and TINYTIM calculations were aligned, scaled, and subtracted to reveal the circumstellar nebulosity. Imperfections in the subtraction process lead to residual artifacts along the diffraction spikes, and saturation effects prevent any study of features within a few pixels (20 AU) of the stars or where column bleeding has occurred. The fundamental contrast limit is set by scattering within the WFPC2 cameras, and improves rapidly with increasing distance from the central object. At $r = 2''$, the scattered light background is already about 7 mag/arcsec² fainter than the integrated brightness of the central point source (Krist, 1995).

3.1. T TAURI

Only the northern component of this binary ($0.7''/100$ AU separation) was detected in the short exposures available. The optical star lies close to an arc of reflection nebulosity which encloses it on the N, S, and E. The arc shows

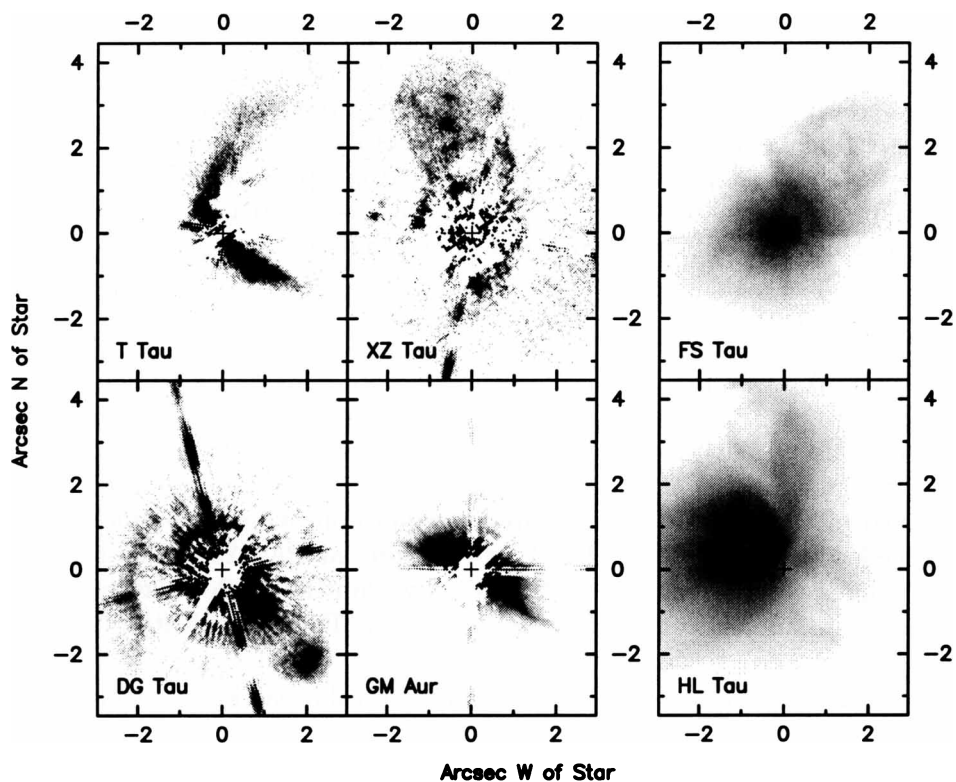


Figure 1. Circumstellar Nebulosity of Six Young Stars. These are PC images, with N up and E to the left. Point-spread functions were subtracted from the four R band images on the left, shown in linear stretch. I band images of FS Tau and HL Tau are shown at right in log stretch.

an approximate symmetry along an axis toward the WNW, the direction of the blueshifted outflow. The arc shape appears similar to models of an illuminated outflow cavity in the circumbinary envelope. For full details, see Stapelfeldt *et al.* (1997a).

3.2. XZ TAURI

Both stars are directly seen in this close ($0.3''/42$ AU) binary. Little or no reflection nebulosity is present. However, an unusual “bubble” of emission nebulosity extends $4''$ (550 AU) NNE of the binary. Knots within the bubble are suggestive of an enclosed jet, but do not align precisely with either star. Kinematic constraints dictate an especially small dynamical age of about 10 years for the bubble. For full details, see Krist *et al.* (1997a).

3.3. FS TAURI (HARO 6-5)

Both stars are also directly seen in this $0.24''$ (34 AU) binary system. Abundant reflection nebulosity extends beyond $5''$ (700 AU) from the binary, where it begins to overlap larger-scale structures associated with FS Tau B. Near the binary the nebula is wispy and complex, with only the suggestion of a symmetry axis. There is no obvious jet structure. A complete discussion will be presented in Krist *et al.* (1997b).

3.4. DG TAURI

Here the central star is directly visible adjacent to three nested arcs of reflection nebulosity. The arcs enclose DG Tau on its N and E sides, and appear offset at distances of $2''$, $5''$, and $10''$ from the star. The innermost arc, seen for the first time in these images, is the smallest and most sharply defined of the group. All three arcs have an approximate symmetry axis aligned with the blueshifted HH jet emerging at PA 225° . This suggests that the arcs represent illuminated edges within the outflow cavity carved by the jet, similar to the situation for T Tau. The multiplicity of arcs is, however, difficult to account for in this scenario.

The DG Tau jet is clearly resolved into several broad knots within $12''$ of the star. The jet has a remarkably large opening angle of 20° , and even the innermost knot shows a clear bow-like morphology at a projected distance of only 400 AU from the star (see also Lavalley, Dougados, and Cabrit 1997). The large radial velocities measured for the DG Tau jet (Solf and Böhm, 1993) suggest that the system is viewed at only a modest inclination angle from the jet axis. In this case we look “down the throat” of the outflow cavity and the jet should appear foreshortened, circumstances which seem in accord with the observed morphology.

3.5. GM AURIGAE

This star is noteworthy for its circumstellar disk mapped in CO rotational emission lines by Dutrey (1997) and Koerner, Sargent, and Beckwith (1993). The WFPC2 images reveal a flattened circumstellar reflection nebula extending symmetrically from the star to radial distances of $3''$ (450 AU) along position angle 60° . The diameter and position angle of the reflection nebula agree well with values derived from the millimeter interferometer observations of the molecular gas disk. Single scattering models using circumstellar disk density distributions strongly suggest that the GM Aur reflection nebulosity arises at the illuminated upper surface of a flared, optically thick disk observed from $\approx 25^\circ$ above its equator plane. Further details will appear in Stapelfeldt *et al.* (1997b).

3.6. SAO 76411A & HDE 283572

These two G-type weak line T Tauri stars possess no significant infrared, millimeter, or polarization excesses. The WFPC2 images show no evidence for circumstellar nebulosity. Our modeling work rules out optically thick disks for these sources unless they are viewed from high latitudes.

4. Results for Entirely Nebulous Objects

4.1. HL TAURI

It had long been assumed that this star was directly visible through an $A_V \approx 3$ mag (Beckwith *et al.* 1990). One of the first and most surprising YSO results obtained with WFPC2 was the complete absence of a visible star in HL Tauri; the “star” turned out to be the reflection nebula’s compact core, only 1” across. The actual star is located by VLA astrometry about 1” SW of the centroid of the optical nebula, and is extinguished by $A_V > 22$ mag. Most of the visible light is scattered within the cavity carved through the surrounding envelope by the blueshifted jet; the disk is only visible via the extinction edge it produces at the base of the reflection nebula. Additional details can be found in Stapelfeldt *et al.* (1995).

4.2. HH 30

HH 30 (Fig 2a.) is perhaps *the* prototype YSO accretion disk system. A flared, optically thick, circumstellar absorption disk, 450 AU in diameter, occults the central star and extends perpendicular to the highly collimated bipolar jets. By comparing the distribution of reflected light at the upper and lower surfaces of the disk to scattering models, important constraints to the disk density distribution can be derived. A detailed description of these results is presented in Burrows *et al.* (1996); a summary appears in Stapelfeldt *et al.* (1996).

HH 30 is the first YSO disk to have its vertical structure clearly resolved. Modeling of the isophotes indicates that the disk is in vertical pressure support, that it has a scale height $H = 15$ AU at $r = 100$ AU, and that its scale height flares with radius more rapidly than expected for a steady-state accretion disk. Optical and mm determinations agree that the disk mass is surprisingly small, only about $10^{-3} M_{\odot}$ for nominal dust properties. This result dictates that the disk should be largely optically thin to its own emergent thermal infrared radiation. The disk mass is not only much smaller than the circumstellar masses typically inferred for HH energy sources (Reipurth *et al.*, 1993), it is so small that steady accretion would consume the system in less than 10^5 years.

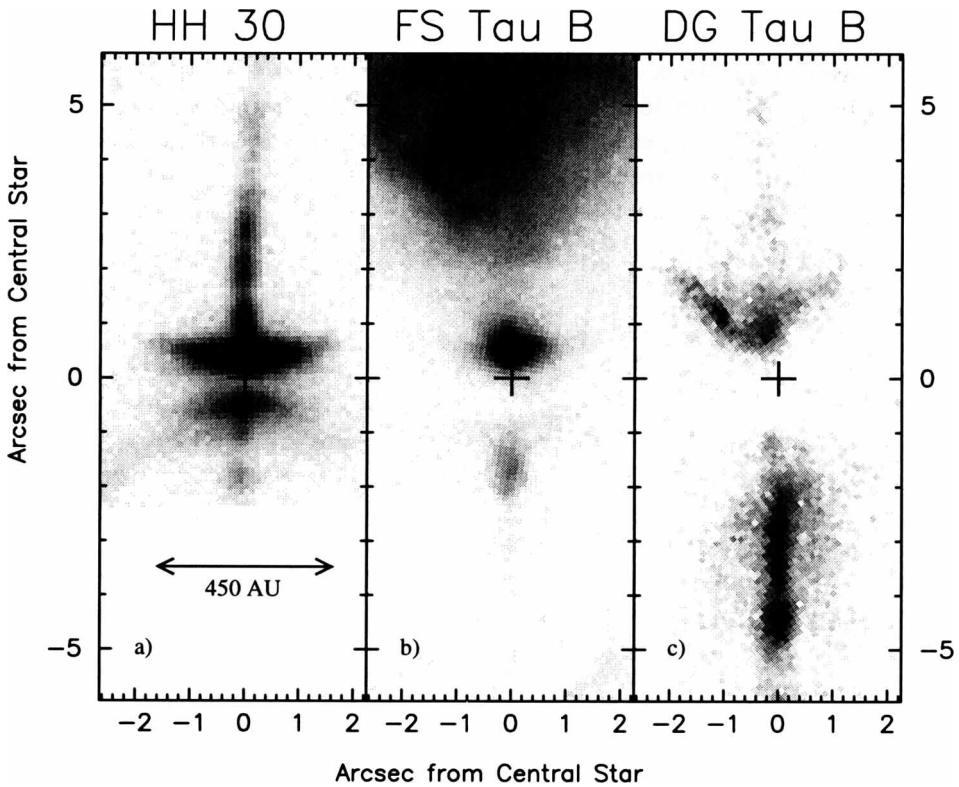


Figure 2. Three HH Energy Sources Resolved as Compact Bipolar Nebulae. These HST WF Camera R band images are shown in log stretch, and have been rotated such that the blueshifted jets are aligned vertically up each panel.

The jet of HH 30 is resolved into many small knots whose spacing along the flow is typically 100 AU. Combined with the measured proper motions of about 200 km s^{-1} , the implication is that new knots emerge from the source every 2-3 years. The jet is exquisitely narrow at its base, with a resolved FWHM of only 25 AU. This observation is difficult to reconcile with inertial collimation provided by the surrounding density distribution, and argues instead for intrinsic collimation very near the central star. The jet brightness fades with distance from the source in a manner consistent with cooling via free expansion. This interpretation is supported by the HST HH 30 emission line images of Ray *et al.* (1996), which show that the $H\alpha/[S \text{ II}]$ ratio smoothly declines with distance along the jet without peaks at the positions of bright knots. HH 30 is the only YSO jet so far where this behavior has been observed.

4.3. FS TAURI B (HARO 6-5B)

HST images of the FS Tau B source region (Fig. 2b) appear similar in several respects to those of HH 30. No stellar point source is present; a compact reflection nebula is seen where the star was presumed to be. At the base of the redshifted jet, a faint companion reflection nebulosity appears, offset from the first one along the jet axis. Both reflection nebulae extend perpendicular to the jet axis for a distance of about 350 AU. They are separated by a dark, slightly curving absorption lane which we identify as the actual circumstellar disk of FS Tau B. Significant structural differences also exist between this system and HH 30. The brightness ratio of the opposing reflection nebulae is larger in FS Tau B, indicating that the system is not so nearly edge-on as HH 30. The dark lane is wider in FS Tau B, which suggests a larger disk mass. Finally, there is an extended cone of reflected light along the blueshifted jet that has no counterpart in the HH 30 system.

The redshifted jet near the faint counter-nebula (lower half of Fig. 2b) shows 3-4 individual knots and has a FWHM of 50 AU. A significant new result is a pattern of transverse “wiggles” in the blueshifted jet at distances 20'' out from the source. This deviation from a cylindrical profile is responsible for the large apparent jet diameter found in lower resolution images of this region by Mundt, Ray, and Raga (1991). A full description of our images, including comparison of disk models and the morphology of the FS Tau B source region, will appear in Krist *et al.* (1997b).

4.4. DG TAURI B

This object lies 1' WSW of DG Tau and drives a redshifted molecular outflow (Mitchell *et al.*, 1994). HST also resolves DG Tau B as a compact bipolar nebula, with no directly visible star. Offset astrometry places the VLA source (Rodriguez, Anglada, and Raga, 1995) within the central dark lane, and offset somewhat toward the reflection nebulosity at the base of the blueshifted jet. Here the central absorption lane is quite wide ($> 1''/140$ AU). Unlike HH 30 and FS Tau B, the scattered light nearest the source is more extended along the jet axis than perpendicular to it. This, and the lack of symmetry between the two reflection nebulae, suggests that optical light is scattered within cleared cavities in a circumstellar envelope. The disk presumably lies embedded within this envelope, and should be revealed via high resolution near-IR imaging. The bright redshifted jet has a FWHM of 50 AU that changes little along its length.

5. Discussion

Disk and jet structures close to the central object are revealed most clearly in the case of nearly edge-on systems such as HH 30. This orientation removes the glare of direct starlight through absorption in the intervening disk material, and allows the disk vertical structure to be seen in silhouette. It would be very useful for disk and jet studies to uncover other nearby YSOs viewed at similarly favorable orientations as HH 30. One way to accomplish this is suggested by the photometric properties of the three compact bipolar nebulae found so far. In Fig. 3, the K magnitude for nearby optically visible YSOs is plotted against the V-K color of each object. Photometry was taken from Kenyon and Hartmann (1995), Gauvin and Strom (1992), Hughes *et al.* (1994), Greene and Young (1992), Vrba, Rydgren, and Zak (1985), and Herbig and Bell (1988). Most of the objects fall in the upper left portion of the diagram, with a large scatter due to luminosity and spectral type variations as well as distance differences between the various star-forming regions. HH 30, FS Tau B, and DG Tau B fall in the lower right portion of this diagram, significantly offset from other nearby YSOs.

The distinctive photometric properties of the compact bipolar nebulae can be understood by considering the effects of increasing circumstellar extinction on the position of a source in this diagram. Moderate amounts of A_V (< 10 mag) will shift a source's position to the right. As the extinction is increased still further, at some point the dominant contribution to the optical light will transition from direct starlight to scattered light. When this point has been reached, the V magnitude of the system becomes much less sensitive to additional increases in A_V . Direct starlight will remain the primary contributor at $2 \mu\text{m}$ up through much larger values of A_V , however, and thus the K magnitude will continue to fade as the extinction increases. This scenario is supported by the photometry and morphology of the three compact bipolar nebulae, and can be summarized as the following hypothesis: *Systems with nearly edge-on disks are best distinguished from their local YSO population by their unusually faint K magnitudes.*

We have used this hypothesis to select additional HST targets which by this reasoning should be revealed as compact bipolar nebulae similar to HH 30. Th 28 in Lupus is an especially promising target, with bipolar jets that show small radial velocities (Krautter, 1986). Another is CoKu Tau/1, for which existing images already suggest that the reflected light is elongated perpendicular to the jet axis (Movsesyan and Magakyan, 1997). It will be interesting to see if these sources prove to be compact bipolar nebulae, and also if their reflected light shows the sharp edges and elegant symmetry of HH 30 or the more diffuse appearance of DG Tau B.

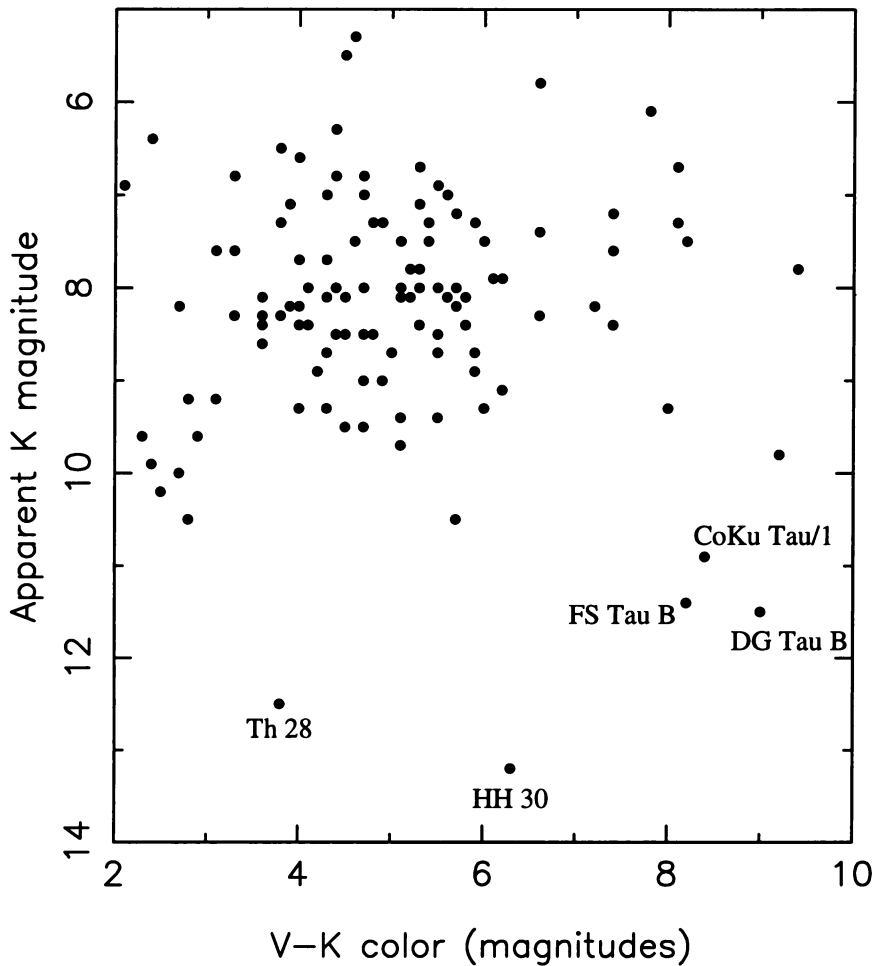


Figure 3. Color-Magnitude Diagram of Selected Nearby YSOs. Optically visible objects with 1.3 mm continuum emission in the Taurus, Chamaeleon, Lupus, and Ophiuchus clouds are included.

6. Future Prospects

Many more YSO imaging studies are now scheduled to occur with HST. These include follow-up observations of HH 30, HL Tau, and T Tau; the first views of the circumbinary disk in GG Tau and the expected absorption disk in Th 28; and a large snapshot survey of T Tauri stars which have millimeter continuum and/or polarization excesses. Near-infrared coronagraphic imaging with NICMOS should provide a new window into the earliest embedded phases of YSO evolution. The next few years promise to be

a period of significant progress in our understanding of the structure and evolution of protoplanetary environments. Updates on our group's work will be available on the WWW at <http://scivax.stsci.edu/~krist/yso.html>.

Acknowledgements: This work was performed under contract to NASA as part of the WFPC2 GTO Science Program. KRS also acknowledges support from the NASA Origins of Solar Systems research program.

References

- Beckwith, S.V.W., Sargent, A.I., Chini, R.S., and Gusten R. 1990, A.J. 99 924
 Burrows, C.J. and the WFPC2 Science Team 1996, Ap.J. 473, 437
 Dutrey, A. 1997 in preparation
 Gauvin, L.S. and Strom, K.M. 1992 Ap.J. 385 217
 Greene, T.P., and Young, E.T. 1992 Ap.J. 395 516
 Herbig, G.H., and Bell, K.R. 1988 Lick.Obs.Bull. 1111 1
 Hughes, J., Hartigan, P., Krautter, J., and Kelemen, J. 1994 A.J. 108 1071
 Kenyon, S.J., and Hartmann, L. 1995 Ap.J.Suppl. 101 117
 Koerner, D.W., Sargent, A.I., and Beckwith, S.V.W. 1993 Icarus 106 2
 Krautter, J. 1986, A.&A. 161 195
 Krist, J.E. and the WFPC2 Science Team 1997a, Ap.J., in press
 Krist, J.E. and the WFPC2 Science Team 1997b, in preparation
 Krist, J.E. 1995 in *Calibrating Hubble Space Telescope: Post Servicing Mission*, STScI Baltimore, p. 311
 Lavalley, C., Dougados, C., and Cabrit, S. 1997 in *Low Mass Star Formation from Infall to Outflow*, Poster Proceedings of IAU Symposium 182, Grenoble, p. 147
 Mitchell, G.F., Hasegawa, T.I., Dent, W.R.F., and Matthews, H.E. 1994 Ap.J. 436 L177
 Movsesyan, T., and Magakyan, T. 1997 in *Low Mass Star Formation from Infall to Outflow*, Poster Proceedings of IAU Symposium 182, Grenoble, (online version only)
 Mundt, R., Ray, T.P., and Raga, A.C. 1991, A.&A. 252 740
 Ray, T.P., Mundt, R., Dyson, J.E., Falle, S., and Raga, A. 1996 Ap.J. 468 L103
 Reipurth, B., Chini, R., Krugel, E., Kresya, E., and Seivers, A. 1993 A.&A. 232 37
 Rodriguez, L.F., Anglada, G., and Raga, A. 1995 Ap.J. 454 L149
 Solf, J., and Böhm, K.-H. 1993, Ap.J. 410 L31
 Stapelfeldt, K.R. and the WFPC2 Science Team 1997a, submitted to Ap.J.
 Stapelfeldt, K.R. and the WFPC2 Science Team 1997b, in preparation
 Stapelfeldt, K.R. and the WFPC2 Science Team 1996, in *Accretion Phenomena and Related Outflows*, Proceedings of IAU Colloquium 163, in press
 Stapelfeldt, K.R. and the WFPC2 Science Team 1995, Ap.J. 449 888
 Vrba, F.J., Rydgren, A.E., and Zak, D.S. 1985 A.J. 90 2074